J_ID: TRIB DOI: 10.1115/1.4027400 Date: 15-April-14 Stage: Page: 1 Total Pages: 7

Lubrication Performance of Nanoparticles-Laden Gas Film in Thrust Bearing Under Noncontact and Contact Conditions

Hongyan Fan
Key Laboratory of Education Ministry for Modern Design and Rotor-Bearing System,
School of Mechanical Engineering,
Xi'an Jiaotong University,
Xi'an 710049, China

Xue Fan
Key Laboratory of Education Ministry for Modern Design and Rotor-Bearing System,
School of Mechanical Engineering,
Xi'an Jiaotong University,
Xi'an 710049, China
e-mail: fanx@mail.xjtu.edu.cn

Zhiru Yang
Key Laboratory of Education Ministry for Modern Design and Rotor-Bearing System,
School of Mechanical Engineering,
Xi'an Jiaotong University,
Xi'an 710049, China

Dongfeng Diao
Key Laboratory of Education Ministry for Modern Design and Rotor-Bearing System,
School of Mechanical Engineering,
Xi'an Jiaotong University,
Xi'an 710049, China;
Institute of Nanosurface Science and Engineering (INSE),
Shenzhen University,
Shenzhen 518060, China
AQ1 e-mail: dfdiao@szu.edu.cn

The nanoparticles-laden gas film (NLGF), which is formed by adding nanoparticles into the gas film, has a potential to increase the load capacity of the gas film and to protect the surfaces of the bearing from severe contact damage. In order to explore the lubrication performance of NLGF, the load capacity in the noncontact state and the friction coefficient in the contact state were studied experimentally by a novel NLGF thrust bearing apparatus. The effects of nanoparticles concentration on the load capacity and the friction coefficient were investigated, respectively. The lubrication performance of NLGF in a 200 start-stop cyclic test was evaluated. The contact surfaces were analyzed by the surface profilometer, scanning electron microscope (SEM), and energy dispersive spectroscopy (EDS). The results showed that NLGF had the enhancement of the load capacity in the noncontact state and possessed the properties of friction reduction and surface protection in the contact state. An optimal nanoparticles concentration of 60 g/m^3 was found, making NLGF have a relative high load capacity in the noncontact state and the lowest friction coefficient in the contact state. With the optimal concentration, the friction coefficient with NLGF kept a low value during the 200 start-stop cyclic test. Then the friction reduction mechanism of NLGF was discussed, and it was inferred that the surface of the disk was covered with a protective film formed by nanoparticles, leading to a lower shear force. This study opens new perspectives of adding nanoparticles into gas bearings to improve the lubrication performance. [DOI: 10.1115/1.4027400]

Keywords: nanoparticles-laden gas film, noncontact, contact, nanoparticles concentration, load capacity, friction coefficient

1 Introduction

Gas bearings with low friction have wide application in the high-speed rotor systems. In actual operation, the resistance capability of the gas film to a sudden impulsive force is low, which could cause severe contact damage at the surfaces of the rotor and the bearing. In order to reduce the probability of such contact, the load capacity of gas film needs to be increased. There are many methods to increase the load capacity of the gas bearing by optimizing surface grooves [1], film profiles [2], and orifice structure [3]. Nevertheless, the direct contact damage between the relative metal surfaces is still severe when the impulsive force is larger than the maximum load capacity. Hence, the surface protection of the gas bearing is necessary. Up to now, there are few methods to realize both the load capacity increase and the surface protection of the gas bearing.

Various nanoparticles used as oil additives to improve the lubrication performance of oil have been studied over past few years. According to previous research, nanoparticles possess the property to enhance the load capacity of lubricating oil [4–6]. Meanwhile, nanoparticles as oil additives exhibit superior friction-reduction and anti-wear properties [7–9] as well as surface mending properties [10]. Moreover, the nanoparticle concentration has a great influence on the friction-reduction properties [11–13]. For the particulate flow lubrication, powder lubrication was extensively studied theoretically [14–16] and experimentally [17,18]. In this lubrication, air acts as carrier fluid transports lubricating particles into the clearance of a bearing, which is barely used to carry the load. The powders, as the main lubricants, can coalesce and transfer a thin lubricating film to reduce friction and wear between two surfaces during relative motion [19]. The above research indicates that nanoparticle additives can be expected to increase the film load capacity for the gas film aerostatic lubrication. Meanwhile, by taking the advantages of powder lubrication, nanoparticle additives can reduce the frictional damage when the bearing surfaces contact with each other.

However, there are few reports on the lubrication performance of gas film with nanoparticle additives, especially about the load capacity enhancement and the friction reduction of the gas bearing at different working states. In the present study, the NLGF was formed by adding SiO_2 nanoparticles into the gas film in a novel thrust bearing to improve the lubrication performance. The effect of nanoparticle concentration on the load capacity of NLGF in the noncontact state and the friction coefficient in the contact state were investigated, respectively, and an optimal nanoparticle concentration was found. With the optimal concentration, the lubrication performance of NLGF in the 200 start-stop cyclic test was evaluated. The contact surfaces were analyzed by the surface profilometer, SEM, and EDS. Finally, the friction reduction mechanism of NLGF was discussed.

2 Experimental Details

2.1 Experimental Apparatus and Method. Figure 1 shows the photograph and schematic diagram of the nanoparticles-laden gas film thrust bearing apparatus, which includes four units: (1) the nanoparticles-gas flow generating unit, (2) the working and measurement unit, (3) the loading unit, and (4) the data acquisition and post processing unit. In the nanoparticles-gas flow

Contributed by the Tribology Division of ASME for publication in the JOURNAL OF TRIBOLOGY. Manuscript received September 24, 2013; final manuscript received March 30, 2014; published online xx xx, xxxx. Assoc. Editor: Robert L. Jackson.

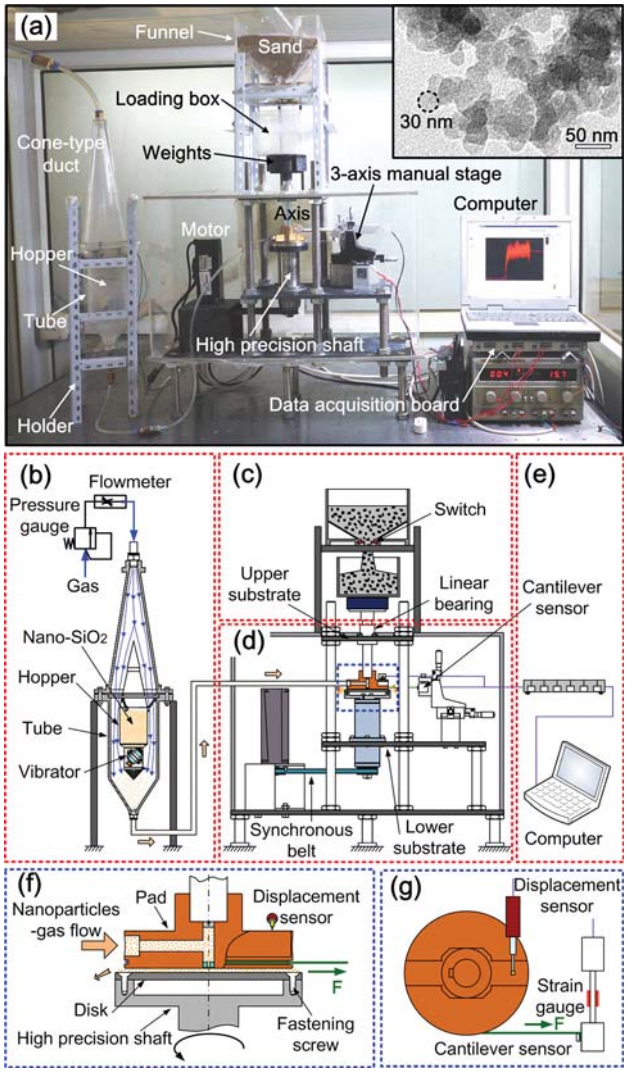

Fig. 1 Photograph and schematic diagram of the nanoparticles-laden gas film thrust bearing apparatus

generating unit (Figs. 1(*a*) and 1(*b*)), the nanoparticles are stored in a hopper equipped with a vibrator. The frequency of the vibrator can be changed by regulating the input voltage and then the amount of the nanoparticles dropped from the hopper in 1 min can be controlled. In this way, the nanoparticles-gas flow with different concentrations can be generated. The working and measurement unit is shown in Fig. 1(*d*). The working bearing consists of two parts: a pad and a disk, as shown in Fig. 1(*f*). The pad is fixed on an axis, which connects to the upper substrate through the linear bearing, and the levelness of the pad is controlled by adjusting the upper substrate. The disk is fixed on a high precision shaft linked with a motor by a synchronous belt. The axial run-out of the motor can be eliminated with the synchronous belt to ensure the running stability of the disk (Fig. 1(*d*)). The end circular run-out error of the disk is adjusted by the fastening screws, and the value is controlled within 5 μm to ensure the running disk is as stable as possible. The measurement parts contain a cantilever sensor and a displacement sensor as shown in Figs. 1(*f*) and 1(*g*). The cantilever sensor with an accuracy of 0.05 N is connected to the pad by a flexible line for detecting the friction torque between the disk and the pad. The displacement sensor with an accuracy of 0.2 μm is fixed on a three-axis manual stage to detect the gas film thickness. The loading unit is composed of a funnel, sand, a switch, a loading box, and weights (Fig. 1(*c*)). By turning on the switch, sand falls into the loading box, and then the load is applied on the pad continuously. The data acquisition and post processing unit includes a data acquisition board and a computer (Fig. 1(*e*)).

In this paper, the noncontact state means that the pad is floated and separated with the disk. In the noncontact state, the load capacity of NLGF is evaluated by the sand weight, which controls the film thickness equal to the initial thickness of pure gas film without nanoparticles. In this process, the motor is off. In the contact state, the pad is dropped and contacted with the rotating disk by stopping the gas supply. The friction torque is obtained from the strain of the cantilever sensor, and then the friction coefficient is calculated with the friction torque and the normal load according to the moment balance theory.

2.2 Experimental Parameter and Procedure. The bearing was an aerostatic thrust bearing with a single inlet port as shown in Fig. 1(*f*). An orifice restrictor of 2 mm in diameter is located at the center of the pad. The material of the pad (90 mm in diameter) was brass with a surface roughness of 0.15 ± 0.02 μm. The material of the disk (100×8 mm) was steel with a surface roughness of 0.20 ± 0.02 μm. There was one pad and a set of disks, so the pad needed to be polished before each test. The working gas was dry and clean compressed air, and the impurity particles with diameter larger than 0.1 μm were filtered out prior to the test. Commercially available spherical SiO_2 nanoparticles with a mean particle size of 30 nm (Fig. 1(*a*)) and a tap bulk density of 0.07 g/ml were used as the additives. Before adding to the gas, the nanoparticles were treated by the ultrasonication and drying process (120 °C for 15 min). After the treatments, the size of the nanoparticles was measured by a laser diffraction particle size analyzer (dry measurement), and the mean diameter was about 2 μm.

In this study, the nanoparticles concentration experiment and the 200 start-stop cyclic test were performed. Both of the two experiments were performed at a gas volume flow rate of 0.05 m^3/min and a working pressure of 0.304 MPa. The nanoparticles concentration experiment was to explore the effects of the nanoparticles concentration on the load capacity of NLGF in the noncontact state and the friction coefficient in the contact state. The range of the nanoparticles concentration was 0–100 g/m^3. In the load capacity tests, the initial load was 70 N. The variations of the film thickness and the load capacity were measured. The friction coefficient tests were performed at a load of 40 N and a bearing rotational speed of 100 rpm. Then, the contact process kept 30 s after the gas supply stopped. During the tests, the film thickness and the friction coefficient were measured. In order to get a precise value of the friction coefficient, the test for each nanoparticles concentration was repeated five times. The start-stop cyclic test was conducted to evaluate the lubrication performance of NLGF during the 200 times contact rubbing between the bearing surfaces. The test was carried out at a load of 40 N and a bearing rotational speed of 100 rpm with an optimal concentration according to the results of the nanoparticles concentration experiment.

After the experiments, the average roughness R_a of the rubbed pad surface was measured by the surface profilometer (Mitutoyo SJ-201P). The surfaces were thoroughly rinsed by ethanol before the measurement. The topography and the elemental component of the rubbed surfaces of the disks were observed and analyzed by SEM and EDS. In order to avoid the effect of the nanoparticles accumulation in the disk center when nanoparticles entered the bearing clearance by the 90 deg turning, the position of 30 mm away from the disk center in radius was chosen to perform the test. Before each test, the surfaces of the disks were cleaned by air purge.

3 Results and Discussion

3.1 Lubrication Performance of Gas Bearing With and Without Nanoparticles. Figure 2 shows the film thickness curve during the load capacity test. The test process was divided into three states: (1) noncontact state, (2) transition state, (3) contact state. Here, the transition state means the process that the pad

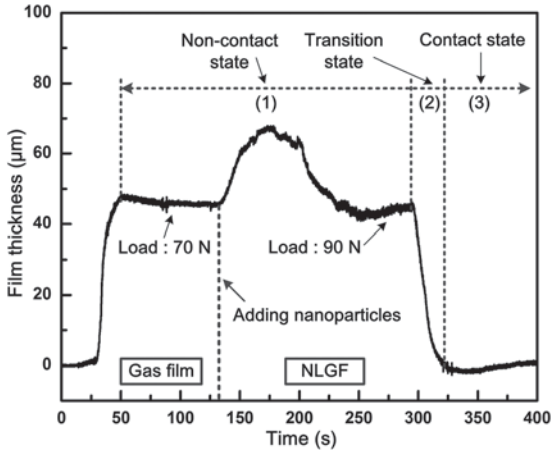

Fig. 2 Variation curve of the film thickness during the load capacity test (nanoparticles concentration: 32 g/m^3)

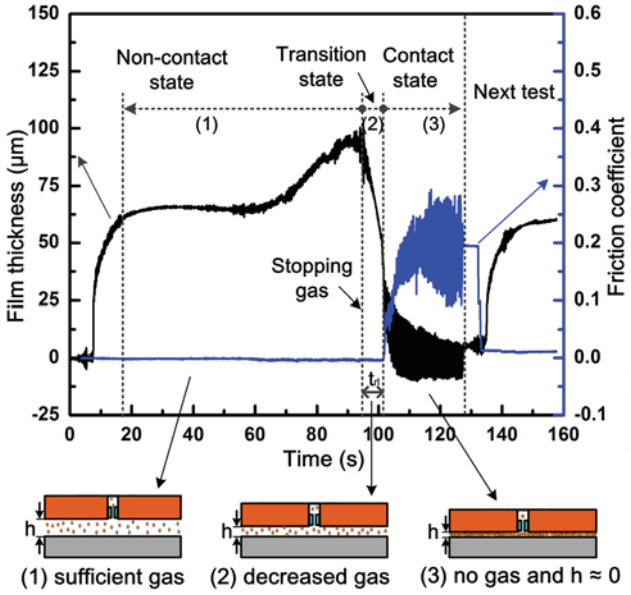

Fig. 3 Variation curves of the film thickness and the friction coefficient during the friction coefficient test (load: 40 N; speed: 100 rpm; nanoparticles concentration: 32 g/m^3)

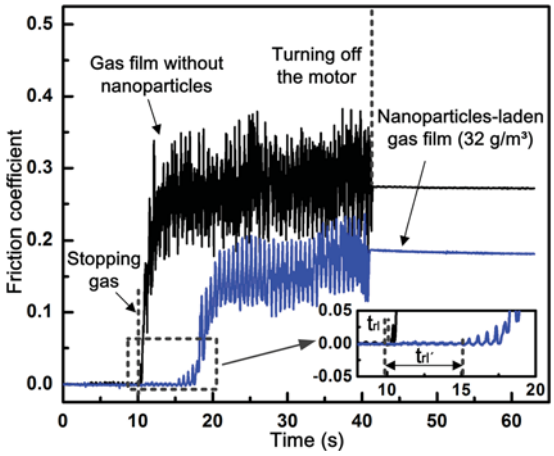

Fig. 4 Friction coefficient curves with pure gas film lubrication and NLGF lubrication in the contact state (load: 40 N; speed: 100 rpm)

descended and finally contacted with the disk after the gas supply stopped. This state was manifested as the decrease of the film thickness. In the noncontact state, the film thickness (h) increased gradually from the initial value of 45 μm to 67 μm after the nanoparticles were added into the gas film. For keeping the film thickness at 45 μm, the load capacity of the gas film increased from 70 N to 90 N after the nanoparticles (concentration of 32 g/m^3) were added. The load capacity of NLGF was increased by 29% in comparison with the pure gas film, which indicates the remarkable enhancement effect of nanoparticles on the load capacity. The mechanism is inferred that nanoparticles can make the bulk viscosity of the NLGF larger than the pure gas film, which leads to a higher load capacity. It should be noted that the nanoparticles were agglomerated because of their high specific surface, and cannot be fully deagglomerated in the air. However, through examining the specific surface area of the agglomerated nanoparticles with a 3H-2000PS2 specific surface and analysis meter of the aperture, it is found that the specific surface area of agglomerated nanoparticles (157 m^2/g) is much larger than that of the 2 μm SiO_2 microparticles (2.92 m^2/g). The results indicate that the agglomerated nanoparticles still have the nanometer effect. Moreover, the film thickness was larger than 45 μm, which was much greater than the mean nanoparticle size of 2 μm. Therefore, the agglomerated nanoparticles do not breakdown the stability of gas film and show the enhancement effect of load capacity.

Figure 3 shows the curves of the film thickness and the friction coefficient during the friction coefficient test. In the noncontact state, the gas supply was sufficient, and the film thickness was stable. Adding nanoparticles into the pure gas film at the time of 50 s, the film thickness increased because of the enhancement effect of NLGF on the load capacity, which was consistent to the result in Fig. 2. Meanwhile, the friction coefficient was zero under the sufficient gas condition. In the transition state, the film thickness decreased gradually with the gas flow rate reducing while the friction coefficient kept unchanged at zero. The time of the transition state was defined as response lag time (t_{rl}). In the contact state, the film thickness returned to about zero due to lack of gas while the curve of the friction coefficient gradually ascended to a stable value.

Figure 4 shows the friction coefficient curves with pure gas film and NLGF lubrication in the contact state. The friction coefficient with pure gas film lubrication ascended instantly when the gas supply stopped. However, the friction coefficient with NLGF lubrication started to increase after 5.6 s. The response lag time of NLGF was much longer. Moreover, the mean stable friction coefficient with the pure gas film lubrication was 0.28, and that with NLGF (32 g/m^3) was decreased to 0.16. The results indicate that the nanoparticles play a role in reducing the friction coefficient. Additionally, the value of the friction coefficient did not return to zero after the motor stopped. This is because the deformation of the cantilever did not reinstate, leading to the static friction force existing between the contact surfaces.

The longer response lag time of NLGF in Fig. 4 can be explained from the perspective of the viscosity. Under the same load capacity, the gas flow rate is inversely proportional to the viscosity of the gas film [20]. The viscosity increases with the nanoparticles concentration [21], so the viscosity of NLGF is larger than that of the pure gas film. Consequently, the gas flow rate of NLGF is lower than that of the pure gas film under the same load capacity. Therefore, in the case of the NLGF, it takes more time for the left gas in the circuit to be exhausted completely after the gas supply stops. Furthermore, the response lag time of NLGF is prolonged, which provides more time to take measures for operators in case of an emergency and reduces the loss caused by the contact damage.

3.2 Lubrication Performance of NLGF With Different Nanoparticles Concentrations. The experimental results of the load capacity and the friction coefficient with different

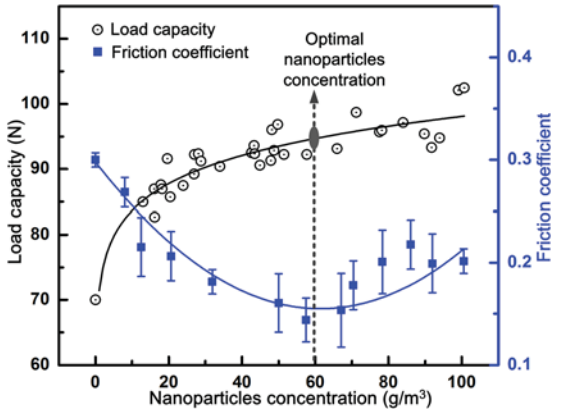

Fig. 5 Load capacity and friction coefficient with different nanoparticle concentrations

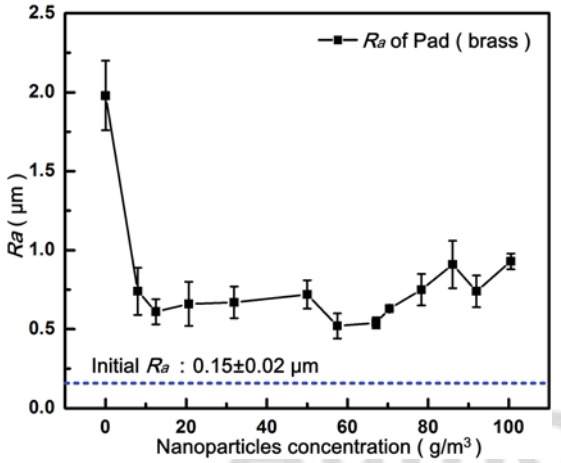

Fig. 6 R_a with different nanoparticle concentrations

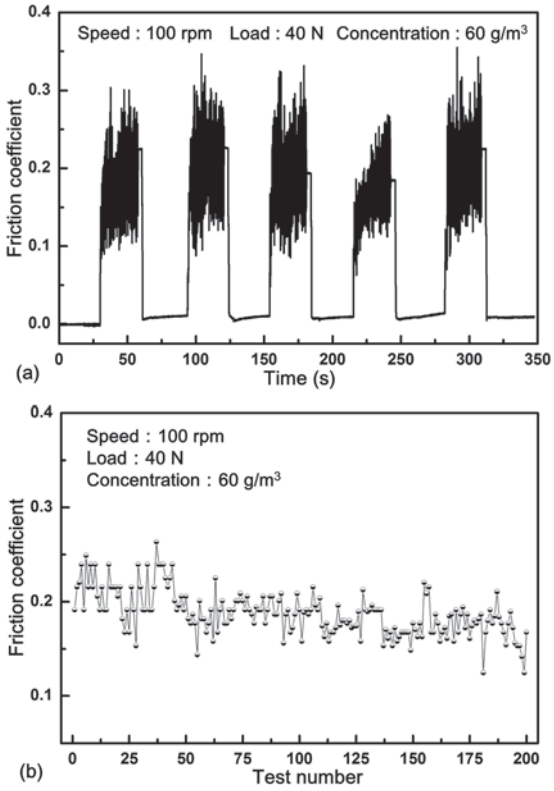

Fig. 7 Variation of the friction coefficient in the start-stop cyclic test

Table 1 Comparison of R_a (the pad)

Lubrication condition	Test cycle	R_a (μm)
Pure Gas film	1	2.03
NLGF (58 g/m^3)	1	0.52
NLGF (60 g/m^3)	200	1.53

nanoparticle concentrations are summarized in Fig. 5. In the noncontact state, the nanoparticles could enhance the load capacity of pure gas film by 21% even at a low value of nanoparticle concentration (13 g/m^3). The load capacity of gas film increased with the nanoparticles concentration increasing. In the contact state, the friction coefficient first decreased gradually with the nanoparticles concentration increasing, and then it rose again after the concentration was higher than a critical value. With the critical nanoparticles concentration of 58 g/m^3, the friction coefficient was reduced by 52% in comparison to the pure gas film. Therefore, the SiO_2 nanoparticles can be taken as good friction reduction additives if their concentration in the gas film is controlled in an optimal range.

To choose a nanoparticles concentration to obtain the optimal lubrication performance of NLGF, the performances both in the noncontact state and in the contact state need to be considered at the same time. In the noncontact state, the efficiency of the load capacity enhancement by increasing the nanoparticles concentration was low when the nanoparticles concentration was higher than 30 g/m^3. In the contact state, the friction coefficient reached the lowest value when the concentration was 60 g/m^3 according to the fitting curve of the experimental results. Therefore, the optimal nanoparticles concentration was 60 g/m^3, which was chosen by taking into account both the load capacity enhancement effect and the friction reduction effect.

The surface morphology of the pad was measured by the surface profilometer after the tests. The surface roughness (R_a) of the pad with different nanoparticles concentrations are shown in Fig. 6. It was found that R_a was 2.03 μm with the pure gas film lubrication. However, R_a was less than 1 μm when the NLGF served as the lubricant. The results suggest that the NLGF can protect the bearing surface with a smaller increase of surface roughness compared with the pure gas film. As the film thickness is very small in the gas bearing, the surface roughness has a great influence on the performance of the gas bearing, which cannot be ignored. Generally, the flow over surfaces with high relative roughness induces pressure fluctuation [22]. The relative roughness is the ratio of the roughness and the film thickness, which is a dimensionless parameter. At a constant value of the gas film thickness in the noncontact state, the relative roughness gets larger with the increasing of surface roughness. The larger the relative roughness is, the more the amplitude of pressure fluctuates, which causes the instability of the running bearing. Under the lubrication of pure gas film, the surface roughness showed a sharp increase after the contact between the bearing surfaces, which affected the working stability of the bearings. Nevertheless, the NLGF could protect the bearing surfaces from severe contact damage in comparison with the pure gas film.

3.3 Start-Stop Cyclic Test. Figure 7(*a*) shows the friction coefficient curve with the NLGF (60 g/m^3) lubrication during five times start-stop tests. By taking the average friction coefficient of each test, the values of the friction coefficient in the 200 start-stop cyclic test were obtained, as shown in Fig. 7(*b*). The friction coefficient did not increase with the test cycle but tended to a steady state gradually. The results illustrate that the NLGF can protect

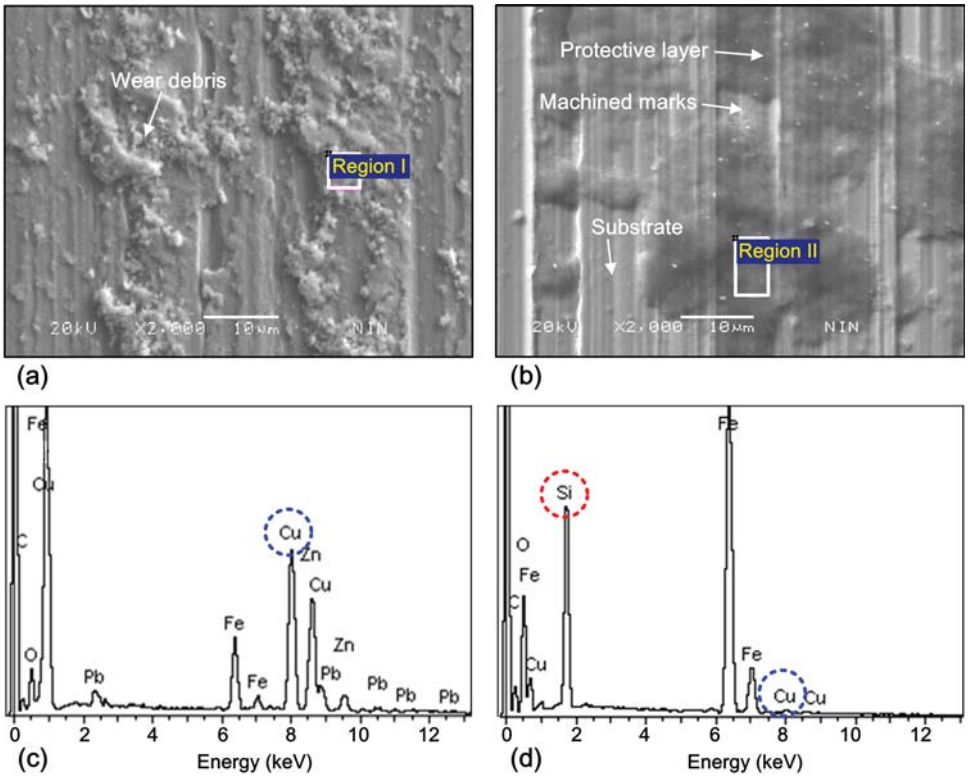

Fig. 8 Analysis results of the worn surfaces on the disks. (*a*) and (*b*): SEM micrographs of the worn surfaces under pure gas film lubrication and NLGF lubrication (nanoparticles concentration: 58 g/m^3), respectively. (*c*) and (*d*): EDS spectra of the region I and II, respectively.

the working surface with a low friction coefficient in numerous contact tests. Hence, the lubrication performance of the NLGF is stable, which helps the NLGF resist the damage for multiple times contacts and, thus, to prolong the working life of the bearing.

The surface roughness of the pad after the 200 start-stop cyclic test was 1.53 μm, as shown in Table 1. R_a increased slightly in comparison to that of one test for NLGF, but still smaller than that of 2.03 μm with the pure gas film. The results showed that the effect of NLGF on the protection of working surfaces was obvious.

3.4 Friction Reduction Mechanism. Figure 8 shows the observation and analysis results of the rubbed surfaces of disks in the contact state. The SEM micrographs of the rubbed surfaces without and with nanoparticles are shown in Figs. 8(*a*) and 8(*b*), respectively. In the case of the pure gas film, a great amount of wear debris was found on the rubbed surface of the disk (Fig. 8(*a*)). To identify the elemental composition of the wear debris, analysis on the EDS result was carried out. The EDS spectrum of region I is shown in Fig. 8(*c*). In the spectrum, except for the element of Fe originated from the steel disk, Cu was another major element detected, which means that the debris was mainly generated by the wear of the brass pad. However, these wear debris did not appear on the rubbed surface lubricated by NLGF (Fig. 8(*b*)). Instead, the surface was covered with a layer, which made the contact surface smoother. Accordingly, Si peak was high in Fig. 8(*d*) indicating that the layer mainly consisted of SiO_2 nanoparticles. Meanwhile, the Cu peak was much weaker in comparison to that in Fig. 8(*c*), which means less wear loss of the brass pad.

According to the above analysis results, we can attempt to explain the friction reduction mechanism. In this study, the spherical nanoparticles may reduce the friction through rolling friction [23], reducing the real area of contact [24] or generating a protective layer [5]. The rolling friction was not observed under the existing detection methods, and it is difficult to occur due to the compaction of the nanoparticles in friction. It is possible that the nanoparticles, as a third body, reduce the real area of contact and then decrease the friction force. Moreover, it was confirmed by the results of SEM and EDS that a layer formed by SiO_2 nanoparticles was found on the surface. The layer on the bearing surfaces eliminates the direct contact between the contact surfaces, which contributes to the decrease of contact damage and, therefore, protects the working surfaces from sever wear. On the other hand, this layer is similar to solid lubricant coatings or transfer films. It is well known that the shear force between the relative sliding surfaces is the metallic bond of the brass pad when the gas film serves as the lubricant. When the layer is formed, the shear for the NLGF occurs within the protective layer, in which the force between nanoparticles is van der Waals bond [25]. It is much weaker than the metallic bond, leading to an easy slip between the pad and the disk, which contributes to a relatively low friction coefficient. However, for the high nanoparticles concentration, the nanoparticles are more likely to cohere into blocks by friction. The larger and harder particles may act as abrasives to scratch the contact surfaces, which result in the increase of friction coefficient. As suggested, an appropriate nanoparticles concentration is needed for the design of NLGF lubrication to effectively increase the load capacity and reduce the friction.

4 Conclusion

The lubrication performance of NLGF was studied experimentally using a novel NLGF thrust bearing apparatus in the noncontact and contact states. The effects of nanoparticles concentration on load capacity and friction coefficient were investigated, and an optimal nanoparticle concentration was found. With the optimal concentration, the lubrication performance of NLGF in the 200 start-stop cyclic test was evaluated. Finally, the friction reduction mechanism of NLGF was discussed. The conclusions from the main results could be drawn as follows:

(1) In the noncontact state, the nanoparticles obviously enhanced the load capacity of the gas film.
(2) In the transition state after the gas supply stopped, the NLGF provided a longer response lag time than the pure gas film.
(3) In the contact state, the NLGF can protect the bearing surfaces from severe damage in terms of reductions in the friction coefficient and the surface roughness. Moreover, the NLGF kept a low friction coefficient during the 200 start-stop cyclic test.
(4) The optimal nanoparticles concentration was 60 g/m^3, with which the NLGF showed a relatively high load capacity in the noncontact state and the lowest friction coefficient in the contact state.

Acknowledgment

The authors would like to acknowledge the support from the National Nature Science Foundation of China (Grant Nos. 51175405 and 91323303), the China Postdoctoral Science Foundation (Grant No. 2012M521755), and the Research Fund for the Doctoral Program of Higher Education of China (Grant No. 20120201110029).

References

[1] Hashimoto, H., and Ochiai, M., 2008, "Optimization of Groove Geometry for Thrust Air Bearing to Maximize Bearing Stiffness," ASME J. Tribol., **130**(3), 031101.
[2] Fesanghary, M., and Khonsari, M. M., 2012, "Topological and Shape Optimization of Thrust Bearings for Enhanced Load-Carrying Capacity," Tribol. Int., **53**, pp. 12–21.
[3] Chen, C. H., Tsai, T. H., Yang, D. W., Kang, Y., and Chen, J. H., 2010, "The Comparison in Stability of Rotor-Aerostatic Bearing System Compensated by Orifices and Inherences," Tribol. Int., **43**(8), pp. 1360–1373.
[4] Rapoport, L., Fleischer, N., and Tenne, R., 2003, "Fullerene-like WS_2 Nanoparticles: Superior Lubricants for Harsh Conditions," Adv. Mater., **15**(7–8), pp. 651–655.
[5] Zhang, M., Wang, X. B., Fu, X. S., and Xia, Y. Q., 2009, "Performance and Anti-Wear Mechanism of $CaCO_3$ Nanoparticles as a Green Additive in Poly-Alpha-Olefin," Tribol. Int., **42**(7), pp. 1029–1039.
[6] Hsin, Y. L., Chu, H. Y., Jeng, Y. R., Huang, Y. H., Wang, M. H., and Chang, C. K., 2011, "In Situ De-Agglomeration and Surface Functionalization of Detonation Nanodiamond, With the Polymer Used as an Additive in Lubricant Oil," J. Mater. Chem., **21**(35), pp. 13,213–13,222.
[7] Li, X. H., Cao, Z., Zhang, Z. J., and Dang, H. X., 2006, "Surface-Modification in Situ of Nano-SiO_2 and its Structure and Tribological Properties," Appl. Surf. Sci., **252**(22), pp. 7856–7861.
[8] Wu, Y. Y., Tsui, W. C., and Liu, T. C., 2007, "Experimental Analysis of Tribological Properties of Lubricating Oils With Nanoparticle Additives," Wear, **262**(7–8), pp. 819–825.
[9] Sánchez-López, J. C., Abad, M. D., Kolodziejczyk, L., Guerrero, E., and Fernández, A., 2011, "Surface-Modified Pd and Au Nanoparticles for Anti-Wear Applications," Tribol. Int., **44**(6), pp. 720–726.
[10] Liu, G., Li, X., Qin, B., Xing, D., Guo, Y., and Fan, R., 2004, "Investigation of the Mending Effect and Mechanism of Copper Nano-Particles on a Tribologically Stressed Surface," Tribol. Lett., **17**(4), pp. 961–966.
[11] Qiu, S. Q., Zhou, Z. R., Dong, J. X., and Chen, G. X., 2001, "Preparation of Ni Nanoparticles and Evaluation of Their Tribological Performance as Potential Additives in Oils," ASME J. Tribol., **123**(3), pp. 441–443.
[12] Li, W., Zheng, S. H., Cao, B. Q., and Ma, S. Y., 2011, "Friction and Wear Properties of ZrO_2/SiO_2 Composite Nanoparticles," J. Nanopart. Res., **13**(5), pp. 2129–2137.
[13] Peng, D. X., Kang, Y., Hwang, R. M., Shyr, S. S., and Chang, Y. P., 2009, "Tribological Properties of Diamond and SiO_2 Nanoparticles Added in Paraffin," Tribol. Int., **42**(6), pp. 911–917.
[14] Heshmat, H., 1995, "The Quasi-Hydrodynamic Mechanism of Powder Lubrication-Part III: On Theory and Rheology of Triboparticulates," Tribol. Trans., **38**(2), pp. 269–276.
[15] Khonsari, M. M., 1997, "On the Modeling of Multi-Body Interaction Problems in Tribology," Wear, **207**(1–2), pp. 55–62.
[16] Jang, J. Y., and Khonsari, M. M., 2006, "On the Role of Enduring Contact in Powder Lubrication," ASME J. Tribol., **128**(1), pp. 168–175.
[17] Klausner, J. F., Chen, D. M., and Mei, R. W., 2000, "Experimental Investigation of Cohesive Powder Rheology," Powder Technol., **112**(1–2), pp. 94–101.
[18] Heshmat, H., 1993, "Wear Reduction Systems for Coal-Fueled Diesel Engines II. Experimental Results and Hydrodynamic Model of Powder Lubrication," Wear, **162**, pp. 518–528.
[19] Wornyoh, E. Y. A., Jasti, V. K., and Higgs, C. F., 2007, "A Review of Dry Particulate Lubrication: Powder and Granular Materials," ASME J. Tribol., **129**(2), pp. 438–449.
[20] Powell, J. W., 1970, *Design of Aerostatic Bearings*, Machinery Publishing Ltd., Brighton, UK.
[21] Enwald, H., Peirano, E., and Almstedt, A. E., 1996, "Eulerian Two-Phase Flow Theory Applied to Fluidization," Int. J. Multiphase Flow, **22**, pp. 21–66.
[22] Zhang, W. M., Meng, G., and Peng, Z. K., 2010, "Random Surface Roughness Effect on Slider Microbearing Lubrication," Micro Nano Lett., **5**(5), pp. 347–350.
[23] Xu, T., Zhao, J. Z., and Xu, K., 1996, "The Ball-Bearing Effect of Diamond Nanoparticles as an Oil Additive," J. Phys. D, **29**(11), pp. 2932–2937.
[24] Ghaednia, H., and Jackson, R. L., 2013, "The Effect of Nanoparticles on the Real Area of Contact, Friction, and Wear," ASME J. Tribol., **135**(4), p. 041603.
[25] Fan, M., 1991, *Engineered Materials Handbook, Ceramics and Glasses*, Vol. 4, ASM International, Metal Park, OH.